Two-Dimensional Scattering by a Homogeneous Gyrotropic-Type Elliptic Cylinder

Abdul-Kadir Hamid[1] and Francis Cooray[2]

[1]Department of Electrical and Computer Engineering, University of Sharjah, Sharjah, UAE
[2]1-7 Rowe Street, Eastwood, NSW 2122, Australia
*corresponding author, E-mail: akhamid@sharjah.ac.ae

Abstract

The separation of variables procedure has been employed for solving the problem of scattering from an infinitely long homogeneous gyrotropic-type (G-type) elliptic cylinder, when a uniform plane electromagnetic wave perpendicular to its axis, illuminates it. Formulation of the problem involves expanding each electric and magnetic field using appropriate elliptic vector wave functions and expansion coefficients. Imposing suitable boundary conditions at the surface of the elliptic cylinder yields the unknown expansion coefficients related to the scattered fields and the transmitted fields. To demonstrate how the various G-type materials and the size of a cylinder affects scattering from it, plots of scattering cross sections are given for elliptic cylinders of different sizes and permittivity/permeability tensors.

1. Introduction

In recent years, research on scattering from two-dimensional (2-D) objects made of gyrotropic-type (G-type) materials has received a great deal of attention, owing to the invention of new materials and technologies, and also since they can be exploited to accomplish unique scattering and/or radiation characteristics. Exact solutions to problems associated with scattering of a normally incident plane electromagnetic wave by circular gyrotropic cylinders have been presented in [1] – [8] and by coaxial circular ferrite cylinders in [9]. Scattering of an obliquely incident plane wave by a gyrotropic circular cylinder was considered in [10], but results presented only for normal incidence of the wave. Two-dimensional scattering of an obliquely incident plane electromagnetic wave from an infinite homogenous anisotropic circular cylinder has been investigated in [11] and [12] using a formulation involving integral equations, with results for a G-type cylinder at normal incidence also included. For analyzing 2-D scattering from a homogeneous gyrotropic cylinder of a non-circular cross section that is excited by a plane wave, a method based on the extended integral equation [13] has been presented in [14], and results have been given for elliptic ferrite cylinders. In [15] and [16], such an analysis has been conducted using a combined-field surface integral equation formulation for 2-D anisotropic objects of arbitrary shape, with results provided for a circular ferrite cylinder also. In [17], 2-D scattering of a transverse electrically polarized normally incident plane electromagnetic wave from a weakly lossy homogeneous gyrotropic elliptic cylinder has been examined, by expressing the electromagnetic fields inside the cylinder using integrals involving Mathieu functions and Fourier series developed in [18], and then employing a first-order Taylor series expansion to calculate Mathieu functions having complex arguments. A formal series solution to the problem of scattering from an infinite homogeneous anisotropic elliptic cylinder excited by a normally incident transverse magnetically polarized plane wave was obtained recently in [19], but when the permittivity and permeability tensors of the anisotropic material referred to the elliptic coordinate axes are biaxial and diagonal.

An exact series solution is reported here for the first time, to the problem of scattering of a plane wave by an infinitely long homogeneous G-type elliptic cylinder, for transverse electric (TE) polarization of the incident wave, when the plane wave is incident normal to its axis. The solution for the transverse magnetic (TM) case is obtained using duality. The originality of this research is in employing the method of separation of variables to obtain a solution to the problem. We have been able to achieve this by expanding all of the fields associated with the problem using appropriate elliptic vector wave functions (involving radial and angular Mathieu functions and their first derivatives) that satisfy the boundary conditions related to the problem, exactly. The solution corresponding to the case of an incident wave of arbitrary polarization can be obtained by exploiting the solutions for the TE and TM cases. When a plane wave illuminated elliptic cylinder is composed of an isotropic, a uniaxial anisotropic, or a biaxial anisotropic material as in [19], the electric field inside it can be expressed using only angular Mathieu functions, similar to that for the electric field of the incident plane wave. However, when the cylinder is made of a G-type material, to express the electric field inside it one needs both the angular Mathieu functions and their derivatives. This is what renders this problem novel and the solving of it more challenging.

The above mentioned solutions have been attainable mainly due to the realization that for a material of gyrotropic type, its permittivity/permeability tensor in relation to a Cartesian or a circular cylindrical coordinate system is identical to

that in relation to the analogous elliptic cylindrical coordinate system.

The exact solution obtained in this paper is beneficial to the electromagnetics community for several reasons. Firstly, it can be applied as a benchmark for validating solutions to analogous problems derived using numerical or approximate procedures (which would have to be done experimentally, otherwise, at a high cost). Secondly, this solution can be used for demonstrating that the method of separation of variables can be employed to solve this type of problems effectively, in contrast to what has been reported in [14] regarding the impossibility of obtaining such a solution. Thirdly, it can be made use of to enhance the collection of canonical solutions for scattering from an assortment of elliptic cylinders, such as those composed of isotropic, uniaxial anisotropic, gyro-electric, gyromagnetic, and gyrotropic-type materials, since there aren't very many articles in the open literature that explore plane wave scattering by elliptic cylinders, using the separation of variables technique. Furthermore, the analysis presented in this paper, enables one to obtain exact solutions to scattering problems involving objects composed of any of the above materials, which could be modeled using elliptic cylinders of proper axial ratios.

To verify the software used for calculations and the analysis, normalized bistatic widths for a TE polarized plane wave illuminated G-type elliptic cylinder with an axial ratio 1.0001 have been calculated first at a number of scattering angles, and compared with comparable results for an analogous G-type circular cylinder given in [12], and shown that they are in superb agreement. Next, we have carried out a similar calculation for a gyromagnetic elliptic cylinder excited via a TM polarized plane wave, compared the results obtained with the equivalent results provided in [14], and shown that the agreement between the results is exceptional.

2. Formulation

Consider an infinitely long elliptic cylinder comprised of a G-type material, excited by a TE polarized plane wave of unit magnetic field amplitude, incident normally to its axis. The semi-major and semi-minor axis lengths of this cylinder are denoted by a and b, respectively, and its axis is along the negative z axis of a Cartesian coordinate system x, y, z, which has the center O of the elliptic face (see Fig. 1) as its origin. The angle ϕ_i is that which the incident plane wave makes with the negative x-axis in Fig. 1. An elliptic co-ordinate system having the same origin O and denoted by u, v, z, is also specified to assist in the analysis. If F denotes the semi-focal length of the above elliptic cylinder, then we can write x and y in terms of u and v as $x = F\cosh u \cos v$ and $y = F\sinh u \sin v$. Even though a time dependence of $\exp(j\omega t)$ has been assumed throughout the paper, it has been suppressed for convenience.

The analysis given below is conducted using elliptic vector wave functions $\mathbf{L}$, $\mathbf{M}$, and $\mathbf{N}$, defined by $\mathbf{L}_{\alpha n}^{(i)} = \nabla\psi_{\alpha n}^{(i)}$, $\mathbf{M}_{\alpha n}^{(i)} = \mathbf{L}_{\alpha n}^{(i)}\times\hat{\mathbf{z}}$, and $\mathbf{N}_{\alpha n}^{(i)} = k^{-1}(\nabla\times\mathbf{M}_{\alpha n}^{(i)})$, where $\psi_{\alpha n}^{(i)}$ is the elliptic scalar wave function, with $\alpha = e$ denoting the even function and $\alpha = o$ the odd function, $\hat{\mathbf{z}}$ is the unit vector in the +z-direction, and k is the wavenumber. The function $\psi_{\alpha n}^{(i)}$ can be written in the form $\psi_{\alpha n}^{(i)} = R\alpha_n^{(i)}(kF,\xi)S\alpha_n(kF,\eta)$, where $R\alpha_n^{(i)}$ is the even or odd radial Mathieu function of the i-th kind and order n of argument $\xi = \cosh u$, and $S\alpha_n$ is the even or odd angular Mathieu function of order n and argument $\eta = \cos v$.

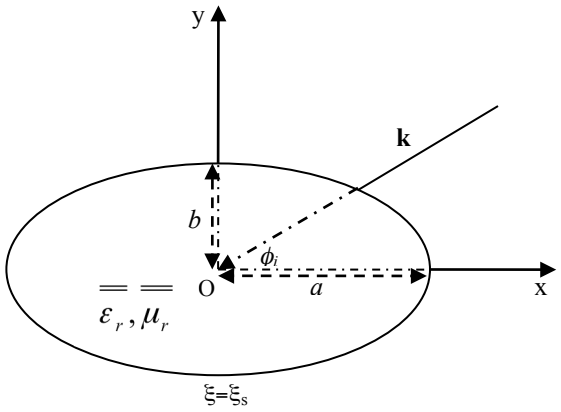

Figure 1: Geometry of the problem.

2.1. Incident and scattered fields

The magnetic fields of the incident and scattered waves can be expanded, respectively, in terms of $\mathbf{N}_{qn}^{(1)}$ and $\mathbf{N}_{qn}^{(4)}$ as [20]

$$\mathbf{H}^{\text{inc}} = \sum_{q=e,o}\sum_{n=0}^{\infty} A_{qn}\,\mathbf{N}_{qn}^{(1)}(c,\xi,\eta) \tag{1}$$

$$\mathbf{H}^{\text{s}} = \sum_{q=e,o}\sum_{n=0}^{\infty} B_{qn}\,\mathbf{N}_{qn}^{(4)}(c,\xi,\eta) \tag{2}$$

in which $\xi = \cosh u$, $\eta = \cos v$, $c = kF$ with k being the wavenumber of the medium exterior to the cylinder, A_{qn} are the known incident field expansion coefficients [21], B_{qn} are the unknown scattered field expansion coefficients, and a bold character denoting a vector. The analogous expansions for the electric fields can be obtained from (1) and (2), by replacing $\mathbf{H}$ by $\mathbf{E}$ and $\mathbf{N}$ by $-jZ\mathbf{M}$, with Z being the wave impedance of the medium exterior to the cylinder.

2.2. Transmitted field

With reference to a right-handed τ, σ, z coordinate system, the tensors corresponding to the G-type material's relative permittivity/relative permeability can be defined as

$$\bar{\bar{\zeta}}_r = \begin{bmatrix} \zeta_{r,\tau\tau} & \zeta_{r,\tau\sigma} & 0 \\ -\zeta_{r,\tau\sigma} & \zeta_{r,\tau\tau} & 0 \\ 0 & 0 & \zeta_{r,zz} \end{bmatrix}_{\tau\sigma z} \tag{3}$$

for $\zeta = \varepsilon, \mu$. The above tensors are generally expressed relative to either a Cartesian coordinate system designated by $\tau = x, \sigma = y$ or a circular cylindrical coordinate system designated by $\tau = \rho, \sigma = \varphi$. Using (A3)-(A14) in [19], it can be shown that the elements of (3) in a Cartesian or a

circular cylindrical coordinate system are identical to those in a corresponding elliptic coordinate system designated by $\tau = u, \sigma = v$. Thus, relative to an elliptic coordinate system, (3) can be written as

$$\bar{\bar{\zeta}}_r = \begin{bmatrix} \zeta_{r,uu} & \zeta_{r,uv} & 0 \\ -\zeta_{r,uv} & \zeta_{r,uu} & 0 \\ 0 & 0 & \zeta_{r,zz} \end{bmatrix}_{uvz} = \begin{bmatrix} \zeta_{r1} & \zeta_{r2} & 0 \\ -\zeta_{r2} & \zeta_{r1} & 0 \\ 0 & 0 & \zeta_{r3} \end{bmatrix}_{uvz}. \quad (4)$$

In view of (4) for $\zeta = \varepsilon, \mu$, the first two Maxwell's equations in the region within the G-type material can be written as

$$\nabla \times \mathbf{E} = -jk_0 Z_0 \bar{\bar{\mu}}_r \cdot \mathbf{H} \quad (5)$$

$$\nabla \times \mathbf{H} = j\,(k_0/Z_0)\bar{\bar{\varepsilon}}_r \cdot \mathbf{E} \quad (6)$$

where k_0 and Z_0 are the wavenumber and the wave impedance in free space. Since the variation of all the field components in the z-direction ($\partial/\partial z$) is zero, using (5) and (6), one can express the field components inside the G-type cylinder as

$$E_u^t = \frac{1}{j\omega\varepsilon_0 h(\varepsilon_{r1}^2 + \varepsilon_{r2}^2)} \left\{ \varepsilon_{r1} \frac{\partial H_z^t}{\partial v} + \varepsilon_{r2} \frac{\partial H_z^t}{\partial u} \right\} \quad (7)$$

$$E_v^t = \frac{1}{j\omega\varepsilon_0 h(\varepsilon_{r1}^2 + \varepsilon_{r2}^2)} \left\{ \varepsilon_{r2} \frac{\partial H_z^t}{\partial v} - \varepsilon_{r1} \frac{\partial H_z^t}{\partial u} \right\} \quad (8)$$

$$H_z^t = \frac{1}{j\omega\mu_0\mu_{r3}h^2} \left[\frac{\partial}{\partial v}(hE_u^t) - \frac{\partial}{\partial u}(hE_v^t) \right] \quad (9)$$

where $h = F\sqrt{\cosh^2 u - \cos^2 v}$. Substituting for E_u^t and E_v^t in (9) from (7) and (8) yields the Helmholtz equation for H_z^t expressed in elliptic coordinates as

$$\frac{\partial^2 H_z^t}{\partial v^2} + \frac{\partial^2 H_z^t}{\partial u^2} + c_{12}^2(\cosh^2 u - \cos^2 v) H_z^t = 0 \quad (10)$$

where

$$c_{12} = \sqrt{c_0\,(\varepsilon_{r1}^2 + \varepsilon_{r2}^2)\mu_{r3}/\varepsilon_{r1}} \quad (11)$$

with $c_0 = k_0 F$. Referring to the solution of (10), the magnetic field within the cylinder can be expressed as

$$\mathbf{H}^t = \sum_{q=e,o} \sum_{n=0}^{\infty} C_{qn}\, \mathbf{N}_{qn}^{(1)}(c_{12}, \xi, \eta) \quad (12)$$

in which C_{qn} are the unknown expansion coefficients. Using (12) in (7) and (8), the electric field within the cylinder can thus be written as

$$\mathbf{E}^t = -\frac{jc_{12}Z_0}{c_0(\varepsilon_{r1}^2 + \varepsilon_{r2}^2)} \sum_{q=e,o} \sum_{n=0}^{\infty} C_{qn} \left[\varepsilon_{r2} \mathbf{L}_{qn}^{(1)}(c_{12}, \xi, \eta) + \varepsilon_{r1}\, \mathbf{M}_{qn}^{(1)}(c_{12}, \xi, \eta) \right]. \quad (13)$$

The involvement of the elliptic vector wave function **L** in (13) renders this problem novel and solving of it more challenging.

3. Analysis

3.1. Imposition of the boundary conditions

Boundary conditions at the elliptic cylinder surface $\xi = \xi_s$ require the continuity of the tangential magnetic and electric fields, given by $H_z^t = H_z^{inc} + H_z^s$ and $E_v^t = E_v^{inc} + E_v^s$. After substituting for the different field components via the above vector wave function expansions expressed in terms of the radial and angular Mathieu functions and their derivatives, then multiplying both sides of each of these equations by an angular Mathieu function of argument c, integrating over v from 0 to 2π and considering the orthogonality of the angular Mathieu functions, yields two sets of equations as in [19], which can be written as

$$\sum_n C_{qn}\, Rq_n^{(1)}(c_{12}, \xi_s) M_{qnw}(c_{12}, c) = \left[B_{qw} Rq_w^{(4)}(c, \xi_s) + A_{qw} Rq_w^{(1)}(c, \xi_s) \right] N_{qw}(c) \quad (14)$$

$$\frac{kZ_0}{k_0 Z} \sum_n C_{qn}\, \varepsilon_{r1}/(\varepsilon_{r1}^2 + \varepsilon_{r2}^2)\, Rq_n^{(1)\prime}(c_{12}, \xi_s) M_{qnw}(c_{12}, c) - \frac{kZ_0}{k_0 Z} \sum_n C_{\tilde{q}n}\, \varepsilon_{r2}/(\varepsilon_{r1}^2 + \varepsilon_{r2}^2)\, R\tilde{q}_n^{(1)}(c_{12}, \xi_s) \widetilde{M}_{qnw}(c_{12}, c) = \left[B_{qw} Rq_w^{(4)\prime}(c, \xi_s) + A_{qw} Rq_w^{(1)\prime}(c, \xi_s) \right] N_{qw}(c) \quad (15)$$

for $w = 0,1,2,\ldots$ and $q = e, o$, with $\tilde{q} = o$ when $q = e$ and vice versa. $Rq_p^{(i)\prime}(c, \xi)$ in (15) is the derivative of the radial Mathieu function of the i-th kind and order p with respect to u, $M_{qnw}(c_{12}, c)$ and $N_{qw}(c)$ in (14) and (15) are defined in [19], and

$$\widetilde{M}_{qnw}(c_{12}, c) = \int_0^{2\pi} S\tilde{q}_n'(c_{12}, \cos v)\, Sq_w(c, \cos v) dv \quad (16)$$

with $S\tilde{q}_n'(c_{12}, \cos v)$ denoting the derivative of $S\tilde{q}_n(c_{12}, \cos v)$ with respect to v. Solving (14) and (15) yields the unknown coefficients B_{qn} and C_{qn}. The solution for the TM case can be obtained in a similar manner, using duality.

3.2. Far fields

By calling to mind that the amplitude of the incident magnetic field is unity, the normalized bistatic width can be written as described in [20], as

$$\frac{\sigma(\phi)}{\lambda} = \left| \sum_{n=0}^{\infty} j^n \left[B_{en} Se_n(c, \cos\phi) + B_{on} So_n(c, \cos\phi) \right] \right|^2 \quad (17)$$

in which $\lambda = 2\pi/k$. Substituting $\phi = \phi_i$ in (17), yields the normalized backscattering width.

4. Results and Discussion

As can be seen from (11), the analysis is dependent only on ε_{r1}, ε_{r2}, and μ_{r3} for the case of TE polarization. From duality, we can see that for the TM polarization situation, the analysis is dependent only on μ_{r1}, μ_{r2}, and ε_{r3}.

Numerical results for G-type elliptic cylinders located in free space, with the definitions of $\bar{\bar{\mu}}_r$ and/or $\bar{\bar{\varepsilon}}_r$ tensors as in (4), are given as normalized bistatic and backscattering widths, when a plane wave of TE/TM polarization is exciting these cylinders. To verify the analysis and the

software used for computations, the normalized bistatic width has first been calculated for a G-type elliptic cylinder with an axial ratio of 1.0001 and a normalized semi-major axis length $k_0 a = \pi/2$, along with $\varepsilon_{r1} = 4$, $\varepsilon_{r2} = 2$, and $\mu_{r3} = 2$, when excited by a TE polarized plane wave incident along the negative x-axis (i.e. at 0^0). In Fig. 2, we have compared these results, with the analogous results computed for an equivalent G-type circular cylinder, obtained using equations (24d) and (25b) of [12], for scattering angles in the range 0^0 to 360^0. As evident from Fig. 2, the results obtained for the elliptic cylinder are in superb agreement with the analogous results for the circular cylinder, validating the veracity of the software used for computations and the analysis, for the TE case. A further proof has been realized by reproducing the results in Figs. 3.3 and 3.4 of [17] associated with elliptic cylinders composed of weakly lossy gyrotropic-type material, but are not shown here, for brevity.

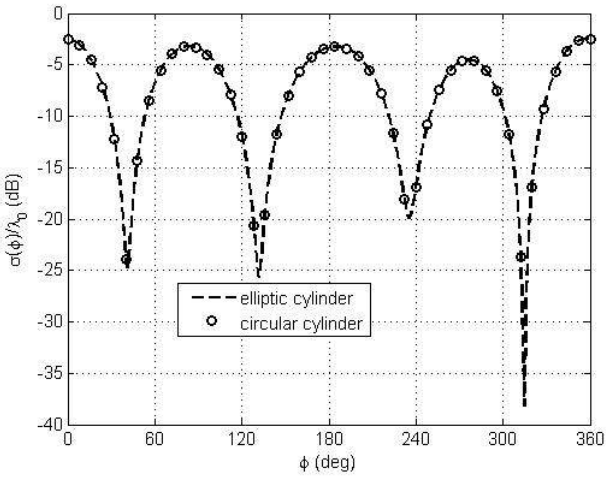

Figure 2: Variation of the normalized bistatic width with the scattering angle, for a G-type elliptic cylinder of axial ratio 1.0001 and $k_0 a = \pi/2$, with $\varepsilon_{r1} = 4$, $\varepsilon_{r2} = 2$, and $\mu_{r3} = 2$, when excited by a TE polarized wave incident at 0^0. Circles show results for an analogous circular cylinder given in [12].

To verify the validity of the analysis and the software used for calculations for the TM case, we have reproduced the results presented in Figs. 6, 8, and 10 of [14] for an elliptic ferrite cylinder of axial ratio $a/b = 2$ and $k_0 a = 1$ excited by a TM polarized plane wave incident at $0^0, 30^0, 60^0$, and 90^0, and the results in Table I of [14], using our formulation, but have presented them in Fig. 3 and Table I, respectively, only for the ferrite cylinder in [14] that has its material parameters described by $\mu_{\text{eff}}/\mu_0 = 0.6786$, $\mu_2/\mu_1 = 0.3571$, and $\epsilon_r = 10$, to save space. $W_1(\phi)$ and $W_2(\phi)$ in Table I, are echo width per wavelength (or normalized bistatic width) given in equation (27a) of [14], and that given in (17), respectively.

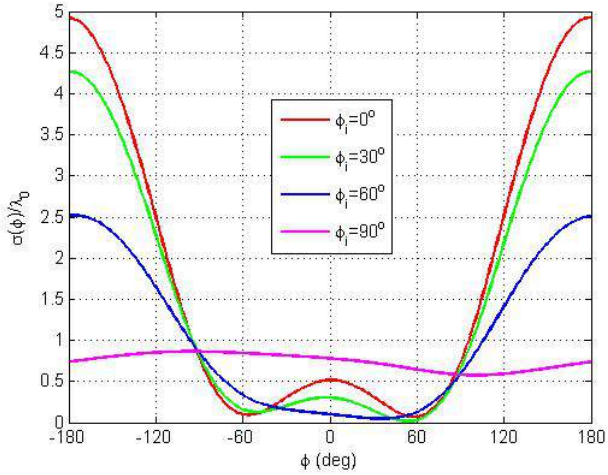

Figure 3: Normalized bistatic width versus scattering angle, when an elliptic ferrite cylinder of axial ratio 2, $k_0 a = 1$, as well as $\mu_{r1} = 7/9$, $\mu_{r2} = -j5/18$, and $\varepsilon_{r3} = 10$, is excited by a TM polarized plane wave, for 4 distinct angles of incidence.

Table I: Echo width per wavelength of the elliptic ferrite cylinder of Fig. 3, whose relative tensor permeability is $\bar{\bar{\mu}}_r$ (columns 2 – 3) or its transpose $\bar{\bar{\mu}}_r^T$ (columns 5 – 6), for a few typical directions of incidence ϕ_i and observation ϕ

(ϕ_i, ϕ)	$W_1(\phi)$	$W_2(\phi)$	(ϕ_i, ϕ)	$W_1(\phi)$	$W_2(\phi)$
$(0^0, 45^0)$	0.1378	0.13781	$(45^0, 0^0)$	0.13812	0.13781
$(0^0, 90^0)$	0.7369	0.73693	$(90^0, 0^0)$	0.73695	0.73693
$(45^0, 0^0)$	0.1458	0.14538	$(0^0, 45^0)$	0.14539	0.14538
$(45^0, 90^0)$	0.6226	0.62262	$(90^0, 45^0)$	0.62263	0.62262
$(90^0, 0^0)$	0.7790	0.77898	$(0^0, 90^0)$	0.77896	0.77898
$(90^0, 45^0)$	0.6866	0.68662	$(45^0, 90^0)$	0.68672	0.68662

According to the reciprocity theorem for scattered waves, interchanging the directions of incidence and observation, and transposing the permittivity/permeability tensor, should retain the observed scattered wave unchanged [22]. We have used this theorem also, to verify the validity of our analysis and software. Results in Table I show that this theorem is satisfied for the cylinder in Fig. 3. When referring to Table I, one can observe that $W_2(\phi)$ in columns 3 and 6 obtained using our formulation are identical, whereas $W_1(\phi)$ in columns 2 and 5 obtained in [14] are not, signifying the better accuracy of our results. Similar results have been obtained for the TE case also, but are not shown here, for brevity.

When discussing the results in Fig. 6 of [14] (which are also given in Fig. 3), it is mentioned in the footnote of [14] page 5, that "*The standard separation of variables procedure cannot be applied to this case because of imperfection of those properties of Mathieu function which concerns orthogonality*". However, we would like to point out that we have been able to calculate the various correlation factors $M_{qnw}(c', c)$ and $\tilde{M}_{qnw}(c', c)$ in (14) and (15), containing angular Mathieu functions and their derivatives with respect to v, of different arguments and orders, successfully, to overcome the difficulties stated in the footnote of [14] page 5, and solve this type of a problem efficiently in this paper, using the standard separation of variables procedure.

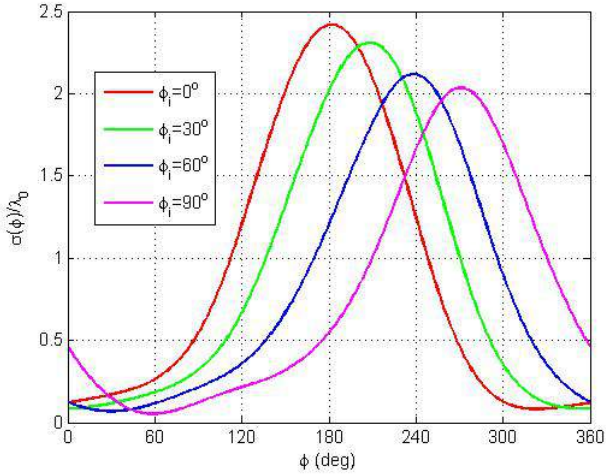

Figure 4: Normalized bistatic width against the scattering angle, when a gyroelectric elliptic cylinder with an axial ratio 2, $k_0a = 0.4\pi$, with $\varepsilon_{r1} = 4$, $\varepsilon_{r2} = -j2$, and $\mu_{r3} = 2$, is excited by a plane wave of TE polarization, for 4 different angles of incidence.

Plots of normalized bistatic widths versus scattering angle are shown in Fig. 4 for a gyroelectric elliptic cylinder of an axial ratio of 2 and $k_0a = 0.4\pi$, together with $\varepsilon_{r1} = 4$, $\varepsilon_{r2} = -j2$, and $\mu_{r3} = 2$, when this cylinder is excited by a TE polarized wave which is incident at 0^0, 30^0, 60^0, and 90^0. For all of the incident angles considered, the patterns resemble each other and the scattering angle at which the maximum normalized bistatic width occurs steadily increases with the incident angle. Also, the magnitude of the peak normalized bistatic width steadily decreases as the incident angle increases.

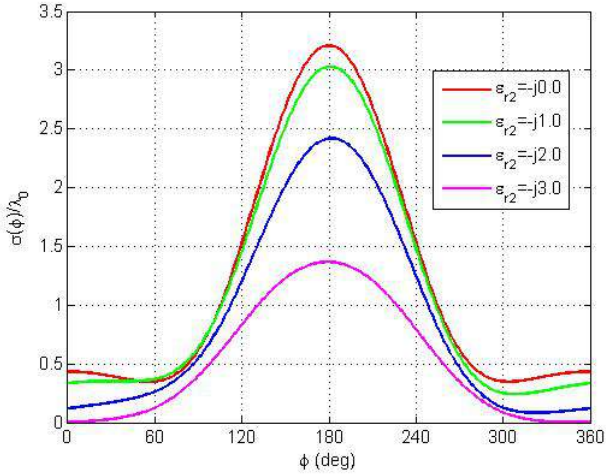

Figure 5: Variation of the normalized bistatic width with the scattering angle, when a gyroelectric elliptic cylinder having an axial ratio of 2 and $k_0a = 0.4\pi$, as well as $\varepsilon_{r1} = 4$, $\mu_{r3} = 2$, and $\varepsilon_{r2} = -j0, -j1, -j2, -j3$, is excited by a plane wave of TE polarization, incident at 0^0.

Figure 5 shows how the normalized bistatic width for a gyroelectric elliptic cylinder of axial ratio 2, $k_0a = 0.4\pi$, with $\varepsilon_{r1} = 4$, $\mu_{r3} = 2$, and for $\varepsilon_{r2} = 0, -j1, -j2, -j3$, changes with the scattering angle, when excited by a TE polarized plane wave incident along the negative x-axis. In Fig. 5, each of the four plots has its maximum at $\phi = 180^0$, and this magnitude (which is the normalized forward scattering width) is largest for $\varepsilon_{r2} = 0$ depicting an uniaxial anisotropic elliptic cylinder, when compared with the analogous magnitudes for the other 3 values of ε_{r2} which characterize 3 gyroelectric cylinders. Also, as ε_{r2} changes from $-j0$ to $-j3$, the normalized bistatic width decreases virtually for all scattering angles, the largest decrease being at $\phi = 180^0$. Out of the 4 curves, the one for $\varepsilon_{r2} = -j0$ is exactly symmetrical about $\phi = 180^0$, while the others are only more or less so.

Results provided in Fig. 6 are for elliptic cylinders having identical dimensions and ε_{r1}, μ_{r3} values as for the cylinders considered in Fig. 5, but with $\varepsilon_{r2} = 0, 1, 2, 3$, when a TE polarized plane wave incident at 0^0 excites them. In this case we observe the symmetry of the curve corresponding to $\varepsilon_{r2} = 0$ characterizing a uniaxial anisotropic cylinder, with its peak at $\phi = 180^0$, and the asymmetry of the other 3 curves for the G-type cylinders, which is more prominent as ε_{r2} changes from 1.0 to 3.0, with the peaks of these 3 curves occurring at scattering angles slightly less than 180^0. Also, the maximum normalized bistatic width magnitude steadily rises with ε_{r2}.

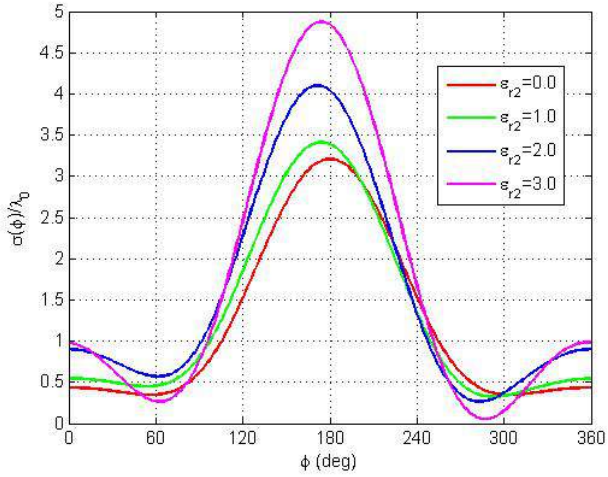

Figure 6: Normalized bistatic width versus scattering angle, when a G-type elliptic cylinder with an axial ratio of 2, $k_0a = 0.4\pi$, as well as $\varepsilon_{r1} = 4$, $\mu_{r3} = 2$, and $\varepsilon_{r2} = 0, 1, 2, 3$, is excited by a plane wave of TE polarization incident at 0^0.

Figure 7 demonstrates the variation of the normalized back-scattering widths against the angle of incidence of a plane wave of TE polarization, for 4 gyroelectric elliptic cylinders of axial ratio 2 and $k_0a = 0.4\pi$, $0.5\pi, 0.6\pi$, 0.7π, with $\varepsilon_{r1} = 4$, $\varepsilon_{r2} = -j2$, and $\mu_{r3} = 2$. All plots are symmetric about $\phi_i = 90^0$ as expected, due to the symmetrical nature of the object, and the magnitude of the highest normalized backscattering width increases with the size of the cylinder. Also, the curves become more oscillatory as the cylinder becomes larger.

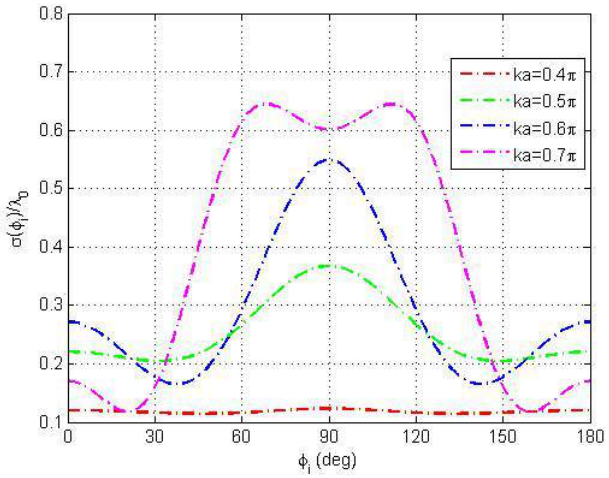

Figure 7: Variation of the normalized backscattering width with the incident angle for gyroelectric elliptic cylinders of axial ratio 2 and 4 different values of $k_0 a$, for $\varepsilon_{r1} = 4$, $\varepsilon_{r2} = -j2$, $\mu_{r3} = 2$, when excited via a TE polarized plane wave.

5. Conclusion

Using the separation of variables procedure, an exact series solution to the problem of scattering from a plane wave excited G-type elliptic cylinder has been obtained. Results have been provided as normalized scattering cross sections for cylinders of various G-type materials and sizes, to demonstrate how the type of gyrotropic material and the size of the cylinder affects scattering from the cylinder. The scattered field is a function of $\bar{\bar{\mu}}$ or $\bar{\bar{\varepsilon}}$ tensor of the G-type substance. Since this tensor for a gyroelectric/gyromagnetic material depends on the applied magnetic dc field, scattering by this type of an object can be controlled using this field. Results provided in Section 4 can be used in the form of benchmarks, to confirm the accuracy of similar results which can be obtained via other methods such as numerical or approximate techniques. The solution has been made efficient by expressing the correlation factors which appear in (14) and (15), in terms of a simple series.

References

[1] V. V. Nikolskii, The simplest case of diffraction of a plane wave on a gyrotropic cylinder, *Radio Eng.* 3: 41 – 46, 1958.

[2] P. M. Platzmann, H. T. Ozaki, Scattering of electromagnetic waves from an infinitely long magnetized cylindrical plasma, *J. Appl. Phys*. 31: 1597 – 1601, 1960.

[3] S. Adachi, Scattering pattern of a plane wave from a magneto-plasma cylinder, *IRE Trans. Antennas Propag.* (*Commun*.) 10: 352, 1962.

[4] S. R. Seshadri, Plane-wave scattering by a magneto-plasma cylinder, *Electron. Lett.* 1: 256 – 258, 1965.

[5] V. A. Es'kin, A. V. Ivoninsky, A. V. Kudrin, The energy flow behavior during the resonance scattering of a plane electromagnetic wave by a magnetized plasma column, *Proc. 8th European Conf. Antennas Propag.* (EuCAP 2014), The Hague, Netherlands, pp. 3321 – 3324, 2014.

[6] W. H. Eggimann, Scattering of a plane wave on a ferrite cylinder at normal incidence, *IRE Trans. Microw. Theory Techn*. 8: 440 – 445, 1960.

[7] J. C. Palais, Scattering from a gyrotropic cylinder, *IEEE Trans. Antennas Propag*. 11: 505 – 506, 1963.

[8] J. C. Palais, Radiation from a ferrite cylinder (part 2), *J. Appl. Phys.*, 35: 779 – 781, 1964.

[9] Y. Chow, Scattering of electromagnetic waves by coaxial ferrite cylinder of different tensor permeablities, *Appl. Sci. Res. B*, 8: 290 – 298, 1960.

[10] S. N. Samaddar, Scattering of plane waves from an infinitely long cylinder of anisotropic materials at oblique incidence with an application to an electronic scanning antenna, *Appl. Sci. Res. B*, 10: 385 – 411, 1962.

[11] J. C. Monzon, N. J. Damaskos, On an integral equation for 2-D anisotropic rod scattering, *Proc. IEEE Antennas Propag. Soc. Int. Symp.*, pp. 1011 – 1014, 1986.

[12] J. C. Monzon, N. J. Damaskos, Two-dimensional scattering by a homogeneous anisotropic rod, *IEEE Trans. Antennas Propag*., 34: 1243 – 1249, 1986.

[13] P. C. Waterman, Matrix formulation of electromagnetic scattering, *Proc. IEEE*, 53: 805 – 812, 1965.

[14] N. Okamoto, Matrix formulation of scattering by a homogeneous gyrotropic cylinder, *IEEE Trans. Antennas Propag.,* 18: 642 – 649, 1970.

[15] B. Beker, K. R. Umashankar, Analysis of electro-magnetic scattering by arbitrarily shaped two-dimensional anisotropic objects: Combined field surface integral equation formulation, *Electromagnetics*, 9: 215 – 229, 1989.

[16] B. Beker, K. R. Umashankar, A. Taflove, Numerical analysis and validation of the combined field surface integral equations for electromagnetic scattering by arbitrarily shaped two-dimensional anisotropic objects, *IEEE Trans. Antennas Propag*., 37: 1573 – 1581, 1989.

[17] S.-C. Mao, F. Wang, Z.-S. Wu, Research on scattering of weakly lossy homogeneous gyrotropic elliptic cylinder, Lecture Notes in Electrical Engineering 206: *Informatics and Management Science III*, W. Du (ed.), Springer-Verlag, London, pp. 19 –23, 2013.

[18] S.-C. Mao, Z.-S. Wu, Scattering by an infinite homogenous anisotropic elliptic cylinder in terms of Mathieu functions and Fourier series, *J. Opt. Soc. Am. A*, 12: 2925 – 2931, 2008.

[19] A.-K. Hamid, F. R. Cooray, Scattering of a plane wave by a homogeneous anisotropic elliptic cylinder, *IEEE Trans. Antennas Propag*., 63: 3579 – 3587, 2015.

[20] A.-K. Hamid, F. R. Cooray, Scattering by a perfect electromagnetic conducting elliptic cylinder, *PIER M*, 10: 59 – 67, 2009.

[21] P. M. Morse, H. Feshbach, *Methods of Theoretical Physics*, Part II, McGraw-Hill, New York, 1953.

[22] J. G. Van Bladel, *Electromagnetic Fields*, McGraw-Hill, New York, pp. 250 – 254, 1964.